Snow Cover on the Tibetan Plateau and Topographic Controls

Duo Chu *, Linshan Liu, Zhoufeng Wang

Posted Date: 3 July 2023

doi: 10.20944/preprints202307.0030.v1

Keywords: MODIS snow cover; SRTM DEM; topographic elements, Tibetan Plateau

Article

Snow Cover on the Tibetan Plateau and Topographic Controls

Duo Chu, [1,2,*] and Linshan Liu [3],Zhoufeng Wang [3]

[1] Tibet Institute of Plateau Atmospheric and Environmental Sciences, Tibet Meteorological Bureau, Lhasa 850000, China;
[2] Tibet Key Laboratory of Plateau Atmosphere and Environment Research, Science & Technology Department of Tibet Autonomous Region, Lhasa 850000, China;
[3] Key Laboratory of Land Surface Pattern and Simulation, Institute of Geographic Sciences and Natural Resources Research, CAS, Beijing 100101, China; liuls@igsnrr.ac.cn(L.L); wangzf@igsnrr.ac.cn(Z.W.)
* Correspondence: chu_d22@hotmail.com; Tel. +86-138-8908-2802

Abstract: Snow cover plays a critical role in the global energy and water cycles. Snow cover on the Tibetan Plateau (TP) provides vital water sources in western China and Himalayan regions in addition to its weather and climate significance. The massive high mountain topography of the TP is main conditions for the presence and persistence of snow cover on the plateau at the mid-low latitudes of the Northern Hemisphere (NH). However, how mountain topography controls snow cover distribution on the TP is largely remain unclear and the relationship is not well quantified. Here, the spatial distribution of snow cover and topographic controls on snow cover on the TP are examined based on snow cover frequency (SCF) derived from MODIS snow cover product (MOD10A2 v5) and digital elevation model (DEM). The results show that snow cover on the TP is spatially unevenly distributed and is characterized by rich snow and high SCF on the interior and surrounding high mountain ranges, and less snow and low SCF in inland basins and river valleys. Snow cover on the TP presents elevation dependence with the higher the altitude, the higher the SCF, the longer the snow cover duration and the more stable the intra-annual variation. Annual mean SCF below 3000 m above sea level (masl) is less than 4% and it reaches 77% above 6000 masl. The intra-annual snow cover variation below 4000 masl features a unimodal distribution, while above 4000 masl it presents a bimodal distribution. The mean minimum SCF below 6000 masl occurs in summer, while above 6000 masl it occurs in winter. Because of differences in solar radiation and water vapor sources, mean SCF generally increases with mountain slopes and it is the highest on the north-facing aspect, whereas the lowest is observed on the south-facing aspect.

Keywords: MODIS snow cover; SRTM DEM; topographic elements; Tibetan Plateau

1. Introduction

Snow cover is a major component of the cryosphere and over 98% of global seasonal snow cover is in the Northern Hemisphere (NH) [1-3]. In winter season, over 40% of land surface in the NH is covered by snow, becoming the fastest temporal and spatial changing surface feature on Earth [4-7]. As a massive elevated land on the Eurasia continent and central region of the High Mountain Asia, the Tibetan Plateau (TP) is the highest and largest mountain region on the world with an average elevation of over 4000 m and covering over 2.5 millions of square kilometers, often called "the roof of the world" or "the third pole of the world" [8-10].

The TP has the largest snow cover extent in the mid-low latitudes of the NH and it is an important component of snow cover in Eurasia. Snow cover on the TP can exit at higher altitude regions throughout seasons and becomes a unique feature in global snow maps [11-13]. Snow cover on the TP affects weather systems and regional climate change through changing surface radiation balance and thermal condition between atmosphere and land surface [14] and snow cover anomalies on the TP has a strong link with Asian monsoon systems [15-16]. On the other hand, as the headwaters of major river systems in Asia, meltwater of snow and ice on the TP plays a

 doi:10.20944/preprints202307.0030.v1

critical role in water supply in the plateau and downstream that over billion people depend on water from these rivers [17-20].

For the large-scale snow cover observations, satellite remote sensing increasingly plays an irreplaceable role due to its advantage of large spatial coverage, various spatial and temporal resolution, low cost and more objectivity. Especially, remote sensing has become the most effective mean to monitor snow cover in the areas with broad extent, complex terrain and difficult access such as the TP. Additionally, coupled with digital elevation model (DEM), it makes possible to reveal spatial distribution of snow cover and topographic controls on snow cover in the mountain regions.

Snow cover in the mountain region is not only closely related to climatic conditions but also vary with topography. The strong altitudinal dependence of snow cover in the mountain region is related to variations in radiation and energy balances [21-22]. Topography has a major effect on snow cover distribution in the Himalayan region [23-24]. Snow cover distribution in the western Himalayans is largely controlled by latitude and altitude [23]. Snow cover variability across the Hindu Kush Himalaya (HKH)region is strongly influenced by topography [23][25] and generally shows altitudinal dependence [26]. The length of snow covered season on the TP appears to be decreasing at lower elevation because of the increase in air temperatures. However, at higher elevations the increase in precipitation appears to compensate for the increase in air temperature such that the snow-free period has decreased [27].

Satellite remote sensing allows detection of spatial-temporal snow cover on the large areas in inaccessible and remote terrain, providing information on a critical component of the hydrological cycle [28]. There is a large spatial variation in snow cover across the Himalayan river basins due to the large climate and altitudinal differences and an obvious relation exists with the elevation [13]. In the western Himalayas, the area covered snow is more than 90% during winter and spring, while it less than 20% of total winter and spring period in most of the area in the eastern Himalayas and Tibetan plateau [13]. Sow cover distribution depends on the terrain height over the TP and the duration for snow persistence varies in different elevation ranges and generally becomes longer with increases in the terrain elevation [29]. Some regional studies were conducted using satellite snow cover data and DEM to reveal the impact of topography on the snow cover distribution on the TP [30-32]and western China [33-36].

The mountain topography of the TP is a main condition and controls for snow cover on the surface, but the quantitative analysis has been lacking so far. Previous research works associated is limited to the northeast [31] and east [32] of the TP. There is a lack of comprehensive study to reveal the relationships between overall terrain conditions of the plateau and spatial distribution of snow cover for entire TP. Therefore, based on the MOD10A2 snow cover products and DEM data, the spatial distribution characteristics of snow cover on the TP is analyzed first, followed by in-depth analysis on the impact of topographic conditions (elevation, slope and aspect) on the spatial distribution of snow cover on the TP. The study is of great significance to understand the spatial distribution of snow resources, snowmelt hydrological effect and responses to climate change, and help lead to better strategy on water resource management in the mountain regions.

2. Materials and Methods

2.1. Study area

The TP is a vast elevated plateau located in the western China at the intersection of Central, South and East Asia and major part of the global mountain regions. The extent for the global mountain areas in the Figure 1 is derived from the reference layer of the Global Mountain Biodiversity Assessment (GMBA) [37].

The TP is surrounded by high mountains and the interior of the plateau is relatively flat. Specifically, The TP is bounded by the Himalayas in the south, Karakorum Mountain in the northwest, western Kunlun and Altun mountains in the north, Qilian Mountains in the

Preprints (www.preprints.org) | NOT PEER-REVIEWED | Posted: 3 July 2023 doi:10.20944/preprints202307.0030.v1

northeast, and Hengduan parallel mountains in the southeast. The interior of the TP consists of plateaus, basins, valleys, lakes, and various small mountains as well as six high mountain ranges (Gangdise, Nyainqentanglha, eastern Kunlun, Tanggula, Bayan Har and Anyemaqen), as shown in Figure 2. The TP is the largest and highest mountain region on the world with average elevation of 4379 m based on 90m SRTM DEM data.

The TP generally can be divided into three major landform units: fold high mountain area in the west and south, vast fault-block plateau and basin area in the interior, and deep gorge and high mountain area in the east. The main part of TP is composed of Tibet Autonomous Region (TAR) and Qinghai Province, with an area of 257.2×10^4 km^2, accounting for about 26.8% of the total land area of China [38-39].

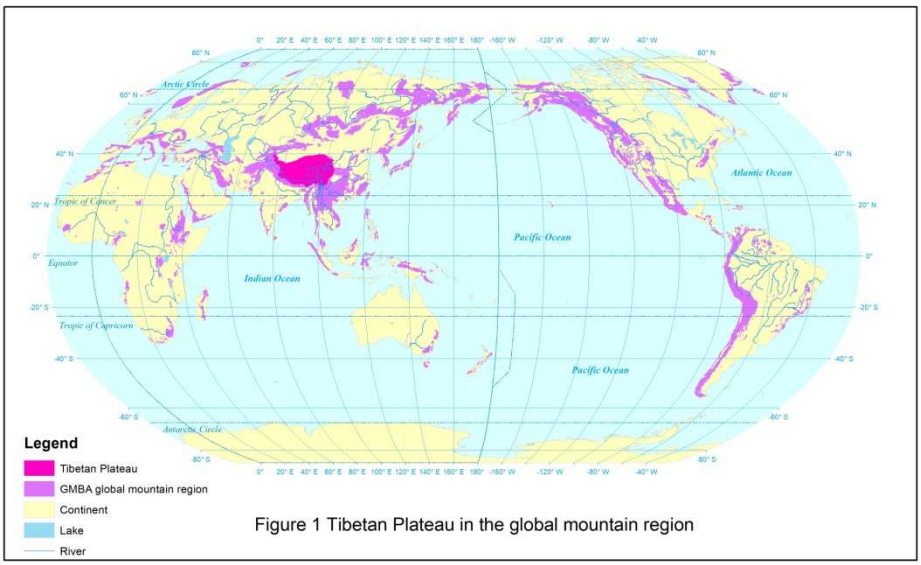

Figure 1 Tibetan Plateau in the global mountain region

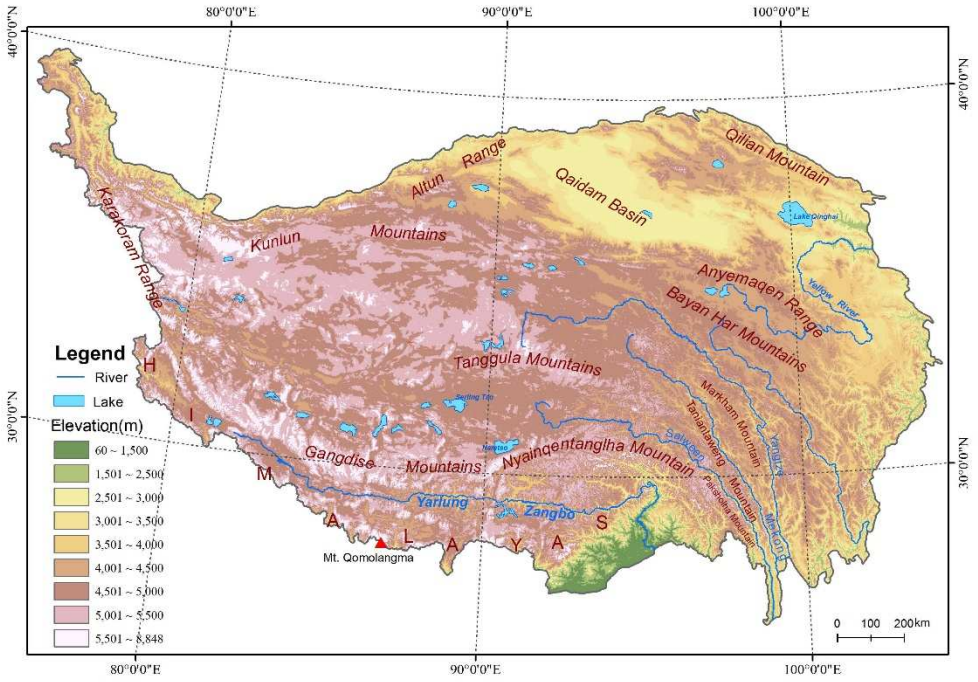

Figure 2. Topography, mountains and main river systems in the TP.

Preprints (www.preprints.org) | NOT PEER-REVIEWED | Posted: 3 July 2023 doi:10.20944/preprints202307.0030.v1

2.2. Data

The snow cover data used in the study is MOD10A2 v005 snow cover products downloaded from the National Snow and Ice Data Center (www.nsidc.org). MOD10A2 is 8-day composite data of MODIS daily snow products (MOD10A1) through 8-day maximum composite method to eliminate cloud obscuration and provides more consistent and cloud-free coverage than daily products [40-41]. The sinusoidal projection is used for the products and the spatial resolution is 500 m.

The studies on accuracy evaluation of MODIS snow cover products have been carried out worldwide since data are available for public. Under the clear sky conditions in the NH, average annual error of MODIS snow cover products is approximately 8% [41-42]. The accuracy of MODIS daily snow cover product (MOD10A1) is 98.2% in the absence of cloud in Xinjiang area in China and snow depth is one of main factors affecting the accuracy of MODIS snow cover mapping [43]. In the northwestern China, MOD10A2 products can effectively eliminate cloud contamination for snow cover classification, and average snow cover detection accuracy is 87.5% [44]. Under clear sky conditions, MOD10A2 has very high accuracy and snow cover mapping accuracy reaches 94% [45]. Pu et al. evaluated the accuracy of MODIS snow cover data by comparing the data with in-situ snow observations in the TP and results show that overall accuracy of MOD10A2 snow cover data is about 90% on the TP area [12]. All above shows that MOD10A2 has a high accuracy for snow cover detection to adequately capture the spatial variability in snow cover of mountain regions in western China and the TP area.

2.3. Methods

2.3.1. Snow cover frequency

The snow cover frequency (SCF) is defined here as percentage of snow cover frequency to examine snow cover process and occurrence frequency in a certain area for a certain time period in the TP by calculating percentage of snow covered pixels in total pixels in MOD10A2 time-series data. Its equation is as follows:

$$\boldsymbol{SCF} = \left[\frac{\mathbf{1}}{\boldsymbol{M}}\sum_{\boldsymbol{i}=\mathbf{1}}^{\boldsymbol{M}}\sum_{\boldsymbol{k}=\mathbf{1}}^{\boldsymbol{D}}\frac{\boldsymbol{N_{ik(1)}}}{\boldsymbol{D}}\right] \times \mathbf{100}\% \quad (1)$$

where, *SCF* is snow cover frequency in percent, $N_{ik(1)}$ is snow cover pixel in k th image of MOD10A2 time-series data in i th year, *M* is the total number of years that MOD10A2 is available. *D* is the total number of MOD10A2 images for year or season. For annual data statistics, k represents the serial number of MOD10A2 images in a year, namely, k =1,2,3,..., *D*=46; for the seasonal statistical analysis, it refers to the serial numbers of MOD10A2 images in spring (March-April-May), summer (June-July-August), autumn (September-October-November) and winter (December-January and February of the next year).

2.3.2. Elevation, slope and aspect data processing

DEM data used in the study is SRTM (Shuttle Radar Topography Mission) DEM that achieved in USGS and downloaded from the National Tibetan Plateau Data Center (http://data.tpdc.ac.cn). The spatial resolution of SRTM DEM is 90 m and is resampled to a spatial resolution of 500 m, consistent with MOD10A2 data. Based on the DEM data, the elevation, slope and aspect data are generated and zoned according to specific terrain and topographic characteristics in the TP. Among them, the elevation is divided into 7 zones with 1 km interval of elevation, namely, below 1 km, 1-2km, 2-3km, 3-4km, 4-5km, 5-6km, and above 6 km of elevation. The slope is divided into four zones, namely, below 5°, 5-10°, 10-20 °, and above 20°. Likewise, the aspect is divided into north-facing slope (315°-45°), east-facing slope (45°-135°), south-facing slope (135°-225°), and west-facing slope (225°-315°) at an interval of 90° and starting from 315° with clockwise, respectively, corresponding to shady slope,

Preprints (www.preprints.org) | NOT PEER-REVIEWED | Posted: 3 July 2023 doi:10.20944/preprints202307.0030.v1

semi-sunny slope, sunny slope and semi-shady slope for mountain terrains. No aspect region (i.e. flat terrain) is represented by "-1".

3. Results

3.1. Spatial distribution of snow cover

3.1.1. Annual mean SCF

Figure 3 shows the spatial distribution of annual mean SCF on the TP from 2001 to 2014. Snow cover on the TP is greatly unevenly distributed, which is generally characterized by rich snow and more perennial snow cover with high SCF on the surrounding and interior high mountains, and less snow and low SCF in the inland plains, basins, and river valleys. Specifically, the Nyainqentanglha and its eastward extending mountain regions in the southeastern Tibet, and Karakoram and western Kunlun Mountains in the northwestern TP, are two regions with the richest snow cover and highest SCF, followed by high mountain ranges such as eastern Kunlun Mountains in the north, Himalayas in the south, Qilian Mountains in the northeast, as well as Tanggula, Anyemaqen and Bayan Har Mountains in the interior and eastern TP. However, mean SCF is low in the vast interior of the plateau except for high mountain ranges. Of which, Qaidam basin and southern Tibetan valley are two areas with the least snow cover occurrence and lowest SCF, followed by Qiangtang Plateau in the northern Tibet, Qinghai Lake basin, and broad eastern region of the Anyemaqen Mountains.

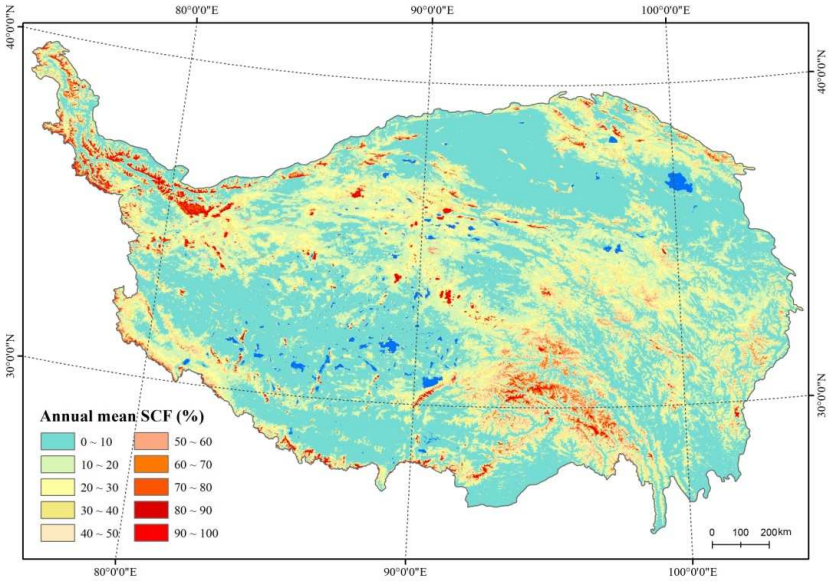

Figure 3. Annual mean SCF on the TP.

Snow cover distribution on the TP is not only related to atmospheric circulation over the plateau, but more importantly it depends on alpine climate and local terrain. Particularly, low temperature condition associated with high elevation is main factor that snow cover sustains on this mid-low altitudes of the NH. In the TP, the high mountain and low-altitude regions are in good agreement with more and less snow cover distributions.

The spatial analysis shows that annual mean SCF on the TP is 15.7%. Of which, the area with SCF <10% accounts for around half of the total TP area (Table 1), mainly distributed in the Qaidam basin, southern regions of Lake Qinghai, middle and lower reaches of Yarlung Zangbo River, and Qiangtang Plateau in northern Tibet. The area with SCF > 60% accounts for only 3.1% of total plateau area and is mainly distributed in the Nyainqentanglha mountains and its southeastern extension, Karakoram, Kunlun, Himalaya, Qilian, Tanggula, Bayan Har and Anyemaqen mountain ranges in surrounding and interior TP. The higher SCF corresponds well with huge mountain ranges. The more

Preprints (www.preprints.org) | NOT PEER-REVIEWED | Posted: 3 July 2023 doi:10.20944/preprints202307.0030.v1

persistent snow cover on the Karakoram and western Kunlun mountains in the northwestern TP is due to westerly disturbance during the winter and early spring, where are the most heavily glaciated regions in the high mountain Asia. In the southeastern TP, high SCF is attributed to more warm moist air that comes from the southern Asia. In contrast, due to huge shielding from the Himalaya and Karakoram mountains[11[[30], most of the interior of the TP has relatively less snow cover although the averaged elevation is beyond 4000 m.

Table 1. Mean SCF on the Tibetan Plateau.

No.	SCF range (%)	SCF (%)				
		Annual	Spring	Summer	Autumn	Winter
1	0-10	49.9	44.2	87.8	47.3	42.1
2	11-20	24.5	20.7	6.6	20.8	25.3
3	21-30	11.2	11.7	2.2	13.0	11.9
4	31-40	5.7	6.9	0.9	8.2	6.2
5	41-50	3.4	4.4	0.5	4.6	4.0
6	51-60	2.1	3.2	0.3	2.6	2.9
7	61-70	1.1	2.8	0.3	1.1	2.3
8	71-80	0.8	2.2	0.3	0.6	2.0
9	81-90	0.9	2.1	0.4	0.6	1.8
10	91-100	0.3	1.6	0.8	1.3	1.5
Mean SCF		15.7	20.9	5.4	17.5	20.6

3.1.2. Mean SCF in spring

The spatial distribution of mean SCF in spring is generally similar to annual mean SCF, presenting that SCF is high in surrounding and interior high mountain ranges, and low in the basin, river valley and Qiangtang Plateau. The mean SCF in spring is 20.9%, which is the highest among four seasons. As shown in Figure 4 (a) and Table 1, the extent of high SCF areas in spring is obviously larger than annual average. The area with annual mean SCF > 50% accounts for 5.2% of total plateau area, while in spring it reaches 11.9%. Since spring is the transition season from winter type to summer type for the atmospheric circulation over the TP, with progressively enhancing of warm moist flow from the southern Asia, snowfall on the plateau increase considerably, bring about more snow cover occurrences on the TP.

Preprints (www.preprints.org) | NOT PEER-REVIEWED | Posted: 3 July 2023 doi:10.20944/preprints202307.0030.v1

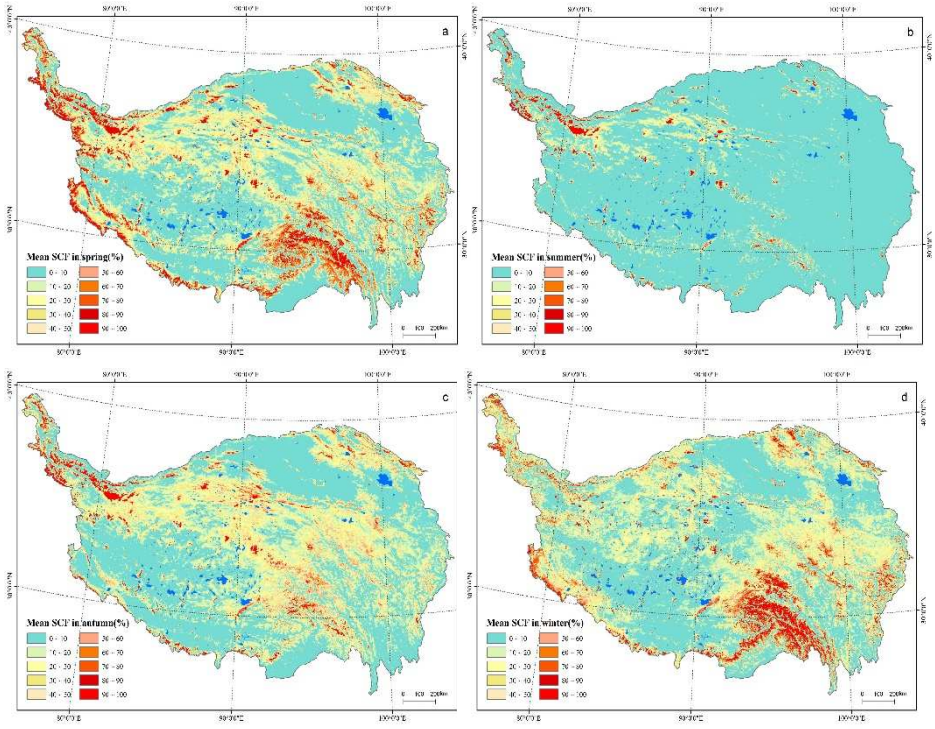

Figure 4. Seasonal mean SCF on the TP in spring (a), summer (b), autumn (c) and winter (d).

3.1.3. Mean SCF in summer

Summer is rainy season for the TP and surface air temperature is above 0°C. Snow covered area on the plateau is very limited and only can be observed in the high mountain ridges and altitudes where the temperature is below 0°C, with mean SCF of 5.4%. The Karakoram in the northwest and Kunlun mountain in the north have higher snow cover frequency relatively, as shown in Figure 4 (b).

3.1.4. Mean SCF in autumn

Compared with summer, snow cover in autumn increases significantly and spatially presents that mean SCF is high in surrounding and interior high mountain ranges, while it is very low in the basin, valley and Qiangtang Plateau. In comparison with spring mean snow cover, a notable increase in mean SCF in autumn is found in higher-latitudes, Nyainqentanglha and Tanggula mountain, and alpine area around Anyemaqen and Bayan Har mountains in southern Qinghai, whereas the increase in SCF is not obvious in autumn at lower latitudes such as southwestern plateau and Himalaya mountains. Mean SCF in autumn is 17.5%, which is lower than mean SCF in spring, primarily related to unobvious increase in snow cover in southern TP compared with spring, as shown in Figure 4 (c). Since autumn is the transition season from summer type to winter type for atmospheric circulation over the TP, with decrease in temperature and cold air becoming more active from the north, the favorable conditions for snowfall and snow cover on the surface make more snow cover occurrences in autumn.

3.1.5. Mean SCF in winter

Like other seasons, winter snow cover on the TP shows high SCF in surrounding and interior high mountain ranges and low SCF in basins and river valleys. However, compared with spring and autumn, major difference in winter is that increase in SCF is obvious in alpine areas in the southeastern TP, especially in alpine regions from Nyainqentanglha to Anyemaqen mountains and Himalayans, as shown in Figure 4 (d). The mean SCF in winter is 20.6%, almost same with spring. The area with mean SCF less than 10% accounts for 42.1% of total TP area, as the least in four seasons due to more snow cover on the surface, and its spatial distribution is generally similar to other

Preprints (www.preprints.org) | NOT PEER-REVIEWED | Posted: 3 July 2023 doi:10.20944/preprints202307.0030.v1

seasons. The main differences show that the increases in snow cover at low latitudes and decline at higher latitudes are more obvious during the winter. In addition to impact of high mountain topography, the spatial distribution of snow cover on the TP is also closely related to atmospheric circulation patterns over the plateau during the winter. The TP is primarily controlled by the westerlies in winter. Low temperature conditions in the interior plateau and high mountains are favorable for the persistence of snow cover on the surface, while southeastern plateau is often disturbed by warm moist airflow from the south, which intersects with cold air from the north, forming weather systems conducive to snowfall.

3.2. Snow cover distribution with elevation

The elevation is main topographic factor affecting spatial distribution of snow cover on the TP. The spatial analysis shows that annual mean SCF below altitude of 3 km TP is very low with less than 3.5%, while above 6 km altitude it reaches 76.8% of total area. There is a quick increasing in mean snow cover between 5 and 6.5 km altitude. Snow cover distribution is variable with elevation at different seasons. The hypsographic curve in Figure 5 shows that the spatial distribution of SCF with elevation in spring and autumn is similar, characterized by the higher the altitude, the higher the SCF. The highest SCF all appear in the area above 6 km altitude with the highest SCF of 86%, and the area below 3 km altitude is little covered by snow. Main seasonal difference in snow cover between 3 km and 6 km altitudes is that mean SCF in spring is slightly higher than that in autumn and the highest difference is observed between 5km and 6 km altitudes with being up to 6%. The highest mean SCF in winter also occurs above 6 km altitude, but it is 32% lower than that in spring and autumn. Compared with other seasons, in winter the snow cover increases obviously at lower altitudes, especially in the area below 4 km altitude, which mainly are attributed to low temperature conditions that are conducive to sustaining snow cover on the TP during winter season. In summer, snow cover on the TP primarily appears at high altitudes above 6 km with SCF of 79.7% on average, while the area below 4 km elevation is little covered by snow.

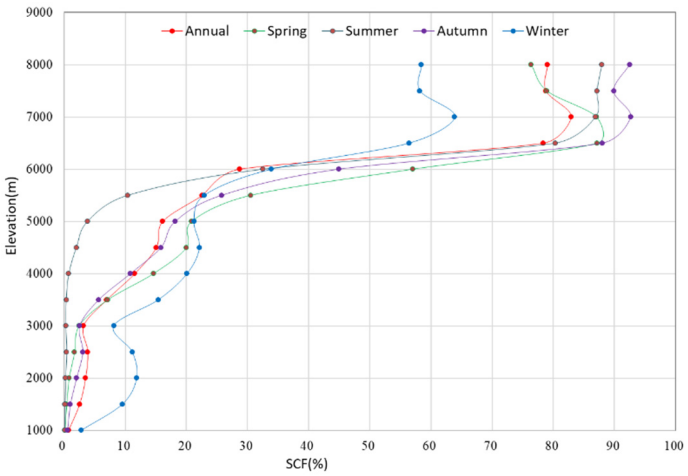

Figure 5. Annual and seasonal mean SCF with elevations on the TP.

In short, mean SCF on the TP increases with elevations in winter season except two elevation zones between 1-3 km. The area with an altitude of 1-2 km is mainly located in the south of the Himalayas. Warm and moist air coming from southern slope of the Himalayas and low temperature in winter often lead to more snow cover on the surface. Whereas, a large area between 2 and 3 km elevation is Qaidam basin in the north, where there is less snow cover in winter, resulting in differences in snow cover distribution between two elevation zones from 1 to 3 km.

The monthly mean snow cover on the TP with elevations is further calculated and results are shown in Figure 6 and Table 2. According to coefficient of variation (CV) given in Table 2, CV is 1.3 in two zones below altitude of 2 km; with the increase in altitude, CV steadily decreases; in elevation zone above 6 km altitude, CV decreases to 0.2, showing that the higher the altitude, the smaller the

Preprints (www.preprints.org) | NOT PEER-REVIEWED | Posted: 3 July 2023 doi:10.20944/preprints202307.0030.v1

CV. It indicates that the higher the altitude, the longer the snow cover duration on the surface, the more stable the intra-annual snow cover variation.

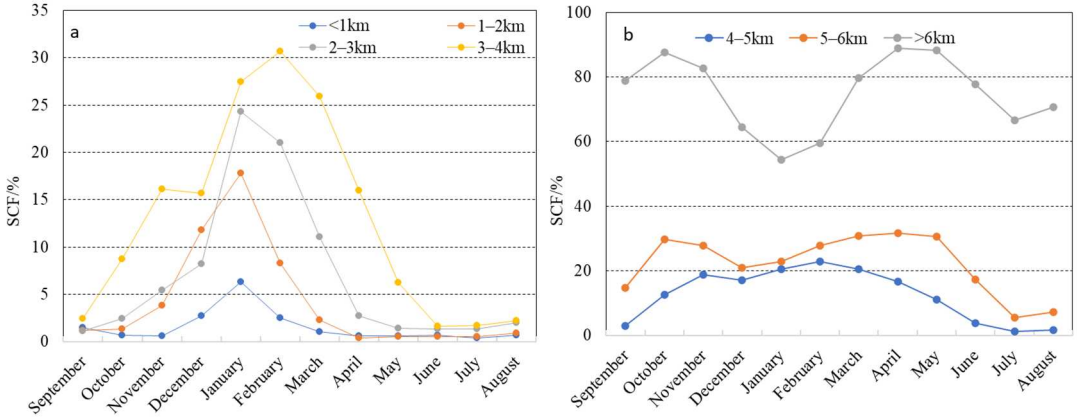

Figure 6. Monthly mean SCF with elevation zones on the TP: below 4 km altitude (a) and above 4 km altitude (b).

Monthly mean SCF in three elevation zones below 3 km are generally same. Snow cover mainly occurs in three winter months and SCF is the highest in January, followed by December and February, while mean SCF in summer months is the lowest with SCF < 1%. In three elevation zones, except for SCF in 1-2km zone being slightly higher than that of 2-3km elevation zone in December and January, mean SCF shows that SCF increases with the elevation. Monthly snow cover variation on the TP in snow season is characterized by that snow cover extent starts to increase from September with the higher the altitude, the more obvious the increase in snow covered area. Mean SCF reaches the peak in January, and then decreases rapidly until it reaches the lowest value in July. Mean SCF below 3 km altitude presents a typical unimodal distribution within snow season, as shown in Figure 6 (a).

Mean SCF at an altitude of 3-4 km is considerably higher than that below 3 km altitude. In this elevation zone, snow cover starts to increase from September and reaches the highest in February, followed by rapid decrease after March and the lowest value in July. Mean SCF variation in this elevation zone also shows a unimodal distribution within snow season as shown in Figure 6 (a). At an altitude of 4-5 km, the highest monthly mean SCF does not occur in winter months but in November with SCF of 25.5%, followed by March with SCF of 24.3%, and the next is February and January, respectively. The intra-annual variation presents a bimodal distribution, with two peaks in November and March, respectively, as shown in Figure 6 (b). Mean SCF at an altitude of 5-6 km is 25.4% and monthly mean SCF increases remarkedly at an altitude of 5-6 km, especially in transition seasons (autumn and spring), and monthly variation of SCF also shows a bimodal pattern.

The highest mean SCF on the plateau occurs in areas above altitude of 6 km with 76.8%, and intra-annual variation in this zone also presents a typical bimodal distribution. At above 6km altitude, the lowest mean SCF occurs in January with 48.0%, while two peaks reach in May and October with 90.8 and 90.6%, respectively. The spatial distribution of snow cover on the TP strongly depends on atmospheric circulation patterns, snowfall and temperature conditions over the TP. Spring and autumn are transition seasons, causing more snowfall processes and snow cover in the high-altitude areas on the plateau. On the other hand, summer is rainy season in the TP, but temperature is low in alpine mountain regions above 6 km altitude and precipitation occurs in the form of snow at high altitude regions, which provides favorable conditions for snow cover on the TP during summer. Low temperature conditions due to high elevations with above 4000 m allow snowfall at any seasons and snow cover can persist at higher altitude regions during all seasons on the plateau [12]. The most of continental glaciers in the TP is fed by snowfall during the summer season [47]. Instead, in winter the TP is mainly affected by cold high pressure systems driven by westerly airflow and weather is mostly clear and sunny with less moisture availability and snowfall events except for plateau-scale disturbances. Snow sublimation under strong insolation and snow blowing due to strong winds

Preprints (www.preprints.org) | NOT PEER-REVIEWED | Posted: 3 July 2023 doi:10.20944/preprints202307.0030.v1

further contributes to decreases in SCF during winter [29]. Sublimation contributes significantly to decreases in SCF during the winter, especially in the areas with thin snow cover. More than half of the snow mass was lost by sublimation in winter [11][47]. Therefore, the lowest mean SCF above 6 km elevation occurs in winter, rather than in summer like other seasons.

Table 2. Monthly mean SCF with elevation zones on the TP.

No.	Elevation range(km)	SCF (%)												CV
		January	February	March	April	May	June	July	August	September	October	November	December	
1	<1	6.2	2.3	0.6	0.2	0.2	0.5	0.3	0.6	1.5	0.7	0.6	2.7	1.3
2	1~2	15.7	7.5	2.2	0.4	0.4	0.4	0.5	0.8	1.2	1.3	3.8	11.8	1.3
3	2~3	10.2	8.2	5.5	1.7	0.8	0.6	0.5	0.7	1.1	2.4	5.4	8.2	0.9
4	3~4	19.6	20.2	18.7	10.8	5.8	1.1	0.8	1.0	2.4	8.7	16.1	15.7	0.8
5	4~5	21.8	23.9	24.3	21.4	16.5	6.7	1.7	2.3	6.3	21.5	25.5	19.7	0.6
6	5~6	23.1	27.6	32.7	35.0	35.1	23.1	8.7	10.0	19.1	35.1	31.2	22.4	0.4
7	>6	48.0	52.2	76.9	90.0	90.8	84.2	76.6	77.8	84.7	90.6	83.7	60.4	0.2
	Mean	20.8	22.8	23.8	21.2	17.9	9.3	3.4	4.1	8.4	20.9	23.5	18.8	

3.3. Snow cover distribution with longitude and latitude

The spatial distribution of snow cover on the TP is affected by geographical latitude and longitude as well through influencing the solar radiation and water budget on the ground. It is generally shows that solar radiation received on the earth surface decrease with increase in latitude, which is in favor of snow cover persistence on the land surface. The precipitation amount in the TP decreases from southeast to northwest, which means that the southeast is more conducive to snowfall and snow cover.

As displayed in Figure 7, the longitudinal distribution of snow cover on the TP is characterized by the higher sow cover frequency in the west and low sow cover frequency in the central and eastern parts of the TP, with obvious seasonal differences between the east and west. The higher SCF is more distinct in the west in spring, while it is more obvious in the east during the winter. In summer, over 10% of annual mean SCF in the northwest of the TP is caused by the perennial snow and ice in the Karakoram and western Kunlun mountains. In winter, the highest mean SCF occurs on the western margin of the TP with over 40%, which is mainly due to westerly disturbance during the winter season.

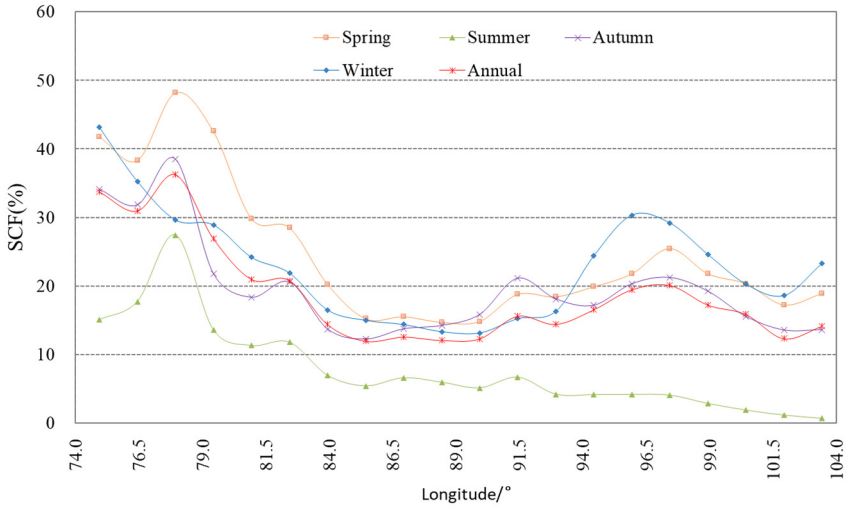

Figure 7. Longitudinal distribution of annual and seasonal mean SCF on the TP.

The latitudinal distribution of snow cover on the plateau generally presents that the increase in snow cover with the latitude is more obvious in the north and south, but this characteristic is not apparent in the central plateau. The increase in snow cover is more obvious in the south during the spring and winter, whereas it is more evident in the north during the winter (Figure 8). In detail, the

Preprints (www.preprints.org) | NOT PEER-REVIEWED | Posted: 3 July 2023 doi:10.20944/preprints202307.0030.v1

areas with more than 10% of mean SCF in summer at high latitudes are mainly found in the western Kunlun and Karakoram Mountains where glaciers and perennial snow cover are located. In the TP, the increase in snow cover with latitude is obvious around below 30.5° and above 38.5°, but it is not prominent between these two latitudes due to more heterogeneity of snow cover distribution.

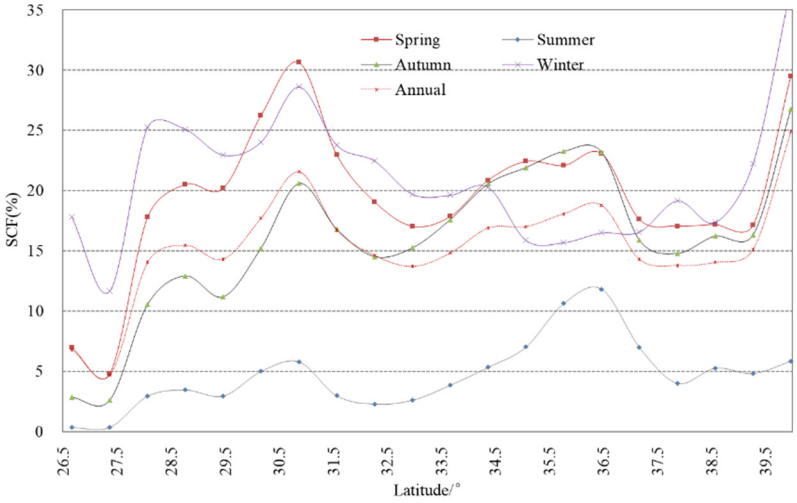

Figure 8. Latitudinal distribution of annual and seasonal mean SCF on the TP.

3.4. Snow cover distribution with aspect

In addition to elevation, aspect, which represents the orientation of slope face, is an important constituent of topography that affects spatial distribution of sow cover on the mountain regions by altering local solar radiation and moisture conditions. Snow cover distribution on the TP with aspects is shown in Figure 9 and Table 3, showing a bimodal distribution in four aspects within the year. In January, mean SCF on the south-facing slope is the lowest (16.7%) and it is the highest on the north-facing slope with 23.9%. After January, snow cover on all aspects increases and the first peak in the year appears in March, with the highest SCF on the north-facing slope (25.9%) and the lowest on the south-facing slope (19.3%). From March to May, snow cover shows decreasing and reaches the lowest value in July. Snow cover starts to increase from August and shows rapid increase from September on the different aspects until November, when it reaches the second peak in the year with little difference from the first peak in spring in terms of peak size.

In contrast, snow cover distribution on the flat terrain without aspects is remarkably lower than that with aspects, and its intra-annual variation presents a unimodal distribution with larger in winter, lower in summer, and intermediate in spring and autumn of transition seasons. Similarly, whether in annual or seasonal average, except for the least snow cover occurring on the flat land without slope orientation, the SCF on the north-facing slope is the highest and it is the lowest on the south-facing slope. The spatially different snow cover distribution on the aspects in the mountain regions is closely related to the redistribution effect of slope orientation on hydrothermal condition in the TP. As we know, south-facing aspects receive more solar radiation, which often enhances snowmelt, resulting in less accumulation on these aspects. However, snow cover on the north-facing areas receives less insolation and thus melts slower than over south-facing areas [21-22]. On the other hand, strong insolation prevails throughout the year due to the low latitude. Sublimation under strong insolation contributes significantly to decreases in SCF on the plateau especial for the areas with thin snow cover [11-12]. North-facing slope receives much less radiation and low sublimation and is favorable for sustaining snow cover on the surface. All these characterize that the high terrain of the plateau affects spatial distribution and temporal variation of snow cover through the changing radiation balance and redistribution of hydrothermal conditions in the mountain regions.

Preprints (www.preprints.org) | NOT PEER-REVIEWED | Posted: 3 July 2023 doi:10.20944/preprints202307.0030.v1

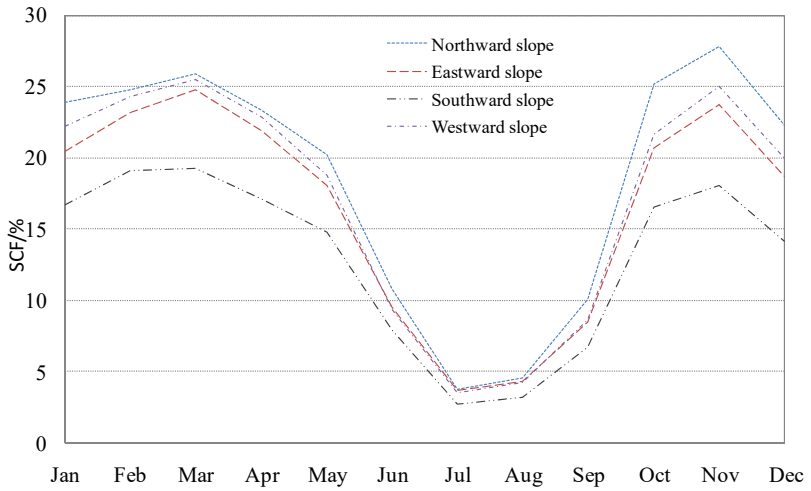

Figure 9. Monthly mean SCF with aspect zones on the Tibetan Plateau.

Table 3. Monthly and seasonal mean SCF with aspects on the TP .

Aspect	SCF (%)																
range(°)	Jan.	Feb.	Mar.	Apr.	May	Jun.	Jul.	Aug.	Sep.	Oct.	Nov.	Dec.	Annual	Spring	Summer	Autumn	Winter
315-45	23.9	24.8	25.9	23.3	20.2	10.8	3.8	4.6	10.1	25.2	27.8	22.3	18.5	23.0	6.2	20.9	23.5
45-135	20.5	23.2	24.8	21.9	18.1	9.5	3.7	4.3	8.5	20.7	23.8	18.7	16.4	21.5	5.7	17.6	20.6
135-225	16.7	19.1	19.3	17.1	14.8	7.9	2.7	3.2	6.7	16.6	18.1	14.2	12.9	17.0	4.4	13.7	16.5
225-315	22.2	24.3	25.5	22.9	18.8	9.3	3.5	4.2	8.6	21.7	25.0	20.0	17.1	22.3	5.5	18.4	22.0
-1	16.9	17.6	17.2	13.8	8.3	2.8	0.6	0.7	1.1	2.7	8.3	14.5	8.6	13.0	1.3	4.0	16.2

3.5. Snow cover distribution with slope

The monthly and seasonal snow cover distribution on the mountain slopes is shown in Table 4. It shows that the SCF on slope below 5° is 16.9% in January and reaches the first peak in February within the year with 23.0%. After that, SCF slowly decreases in months of spring and reaches the lowest level in July, while its second peak appears in October with 19.4%. The intra-annual variation shows a typical bimodal distribution, as shown in Figure 10. Monthly variation of snow cover on three slope zones above 5° is similar to that slope below 5° as described above, with all presenting bimodal distribution, but timing of peak occurrence is delayed by a month (in March and November, respectively). The mean SCF on the slope above 20° is 30.1% in January and the peak is in March with 34.3%. Snow cover increases with slope in months of winter and spring, while it is not obvious in other months. Moreover, on the higher slope the decreasing rate of snow cover from the peak in March to the lowest level in July is faster, while the difference in increasing rate of snow cover from July to November is not noticeable on the different slopes, but changes in snow cover on the slope less than 5° is lower than other slope zones.

In terms of annual average, the SCF on the slope below 5° is the least among four slope zones, with an annual average of 12.7%, and presents that the SCF increases with terrain slope. Annual mean SCF on 5-10° slope zone is 18.4%, while the highest mean SCF of 21% is found on the slope zone above 20°. In terms of seasonal distribution of snow cover on the slope, the SCF on the slope below 5° is the lowest, and in spring the snow cover on 10-20° slope zone is the highest with SCF of 28.1%. In autumn, the highest SCF appears on the slope zones between 5-20°, with around 20%, and in summer the highest SCF appears on 10-20°slope zone. In winter, the highest SCF appears on the slope zone above 20° with SCF of 30.4%. In conclusion, in different slope zones, annual and seasonal mean SCF on the slope below 5° are the lowest, and presents that the SCF is higher on higher slope during winter and spring seasons, but it is not prominent in other seasons.

Preprints (www.preprints.org) | NOT PEER-REVIEWED | Posted: 3 July 2023 doi:10.20944/preprints202307.0030.v1

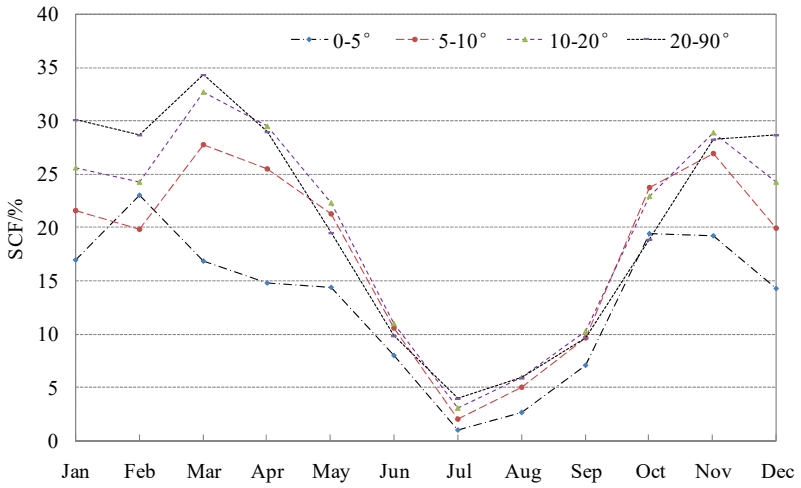

Figure 10. Monthly mean SCF with slope zones on the TP.

Table 4. Monthly and seasonal mean SCF on the slope zones in the TP .

Slope range(°)	SCF (%)																
	Jan.	Feb.	Mar.	Apr.	May	Jun.	Jul.	Aug.	Sep.	Oct.	Nov.	Dec.	Annual	Spring	Summer	Autumn	Winter
0-5	16.9	23.0	16.8	14.8	14.4	8.0	1.0	2.6	7.1	19.4	19.2	14.3	12.7	15.3	4.0	15.1	16.2
5-10	21.6	19.8	27.7	25.5	21.3	10.6	2.0	5.0	9.6	23.7	26.9	19.9	18.4	24.7	6.4	20.0	21.8
10-20	25.6	24.2	32.7	29.5	22.3	11.0	3.0	5.9	10.2	22.9	28.9	24.2	20.6	28.1	7.2	20.6	26.0
20-90	30.1	28.7	34.3	29.0	19.5	9.8	4.0	5.9	9.6	18.9	28.3	28.7	21.0	27.4	6.9	18.8	30.4

Based on the analysis above, the spatial distribution of snow cover on the four aspects along different slopes is further investigated. On the north-facing aspect, snow cover with slope less than 5° is much smaller than that of other slopes, and its intra-annual variation is relatively smooth compared with other slopes. As given in Table 5, mean SCF in January is 17.2% for slopes below 5°, while it reaches 41.9% for slopes above 20°, and it is 25.4% and 33.4% for slopes below 5-10° and 10-20°, respectively. The monthly SCF on the slope below 20° shows a bimodal distribution, with two peaks in November and March, respectively, and the higher the slope, the more typical the bimodal patterns. However, on the slope above 20°, mean SCF presents a unimodal distribution that it is high in winter, low in summer and intermediate in spring and autumn, as shown in Figure 11. On the north-facing aspect, there is a pattern that the higher the slope, the higher the snow cover frequencies in winter and spring, but it is not obvious in other seasons. In snow season, there is no noticeable differences in snow cover on the different slopes between rapid snow accumulation period from September to November and rapid melting season from March to July in the TP.

On the east-facing aspect, mean SCF on the different slope zones is less than that of north-facing aspect. The mean snow cover on the slope below 5° is 16.3% in January, and it is 19.8% in October as the maximum, while snow cover on slope above 20° is 28.3% in January, and the maximum occurs in March with 32.4%. In this slope, snow cover on the slope above 20° increases rapidly from September to November, followed by slow increase until March; after reaching an annual peak in March, snow cover then rapidly decreases, showing a unimodal distribution for intra-annual variations. In other slopes, intra-annual variation in snow cover presents a bimodal distribution, and two peaks generally appear in November and March, and the greater the slope, the more obvious the bimodal distribution pattern. In snow season, there is no distinct difference in snow cover variation in different slopes during snow accumulation period before the peak in autumn and the melting period after the peak in spring. The greater the slope, the more abundant the snow cover on the slope is only found in winter season.

On the south-facing aspect, mean SCF on the different slope zones is less than that of other aspects. Mean SCF on the slope below 5° is 15.9% in January and the maximum is 18.5% in October, while on the slope above 20° it is 19.4% in January and the maximum reaches 26.4% in March.

Preprints (www.preprints.org) | NOT PEER-REVIEWED | Posted: 3 July 2023 doi:10.20944/preprints202307.0030.v1

Monthly mean SCF on the different slope zones on the south-facing aspect presents a bimodal distribution, and two peaks on the slope below 5° appear in October and February, while on the slope zones above 5° the two peaks occur in November and March, which means that intra-annual SCF peaks occur one month later on the higher slope zones (Table 5 and Figure 12). Moreover, the higher the slope, the higher the mean SCF is only found in winter and early spring, whereas this pattern is no obvious on the different slope zones during snow accumulation and melting period.

On the west-facing aspect, mean SCF on the different slope zones is higher than that of southward aspect, but it is lower than that of northward aspect and slightly higher than that of eastward aspect. The intra-annual variations in snow cove on the westward aspect is similar to that of other slope directions, showing that SCF on the slope zone below 20° presents bimodal distribution, while on the slope zone above 20° it presents unimodal distribution. On the westward aspect, monthly SCF on the slope zone below 5° is lower than that of other slope zones, and two peaks occur in February and November, with 19.2% and 20.6% respectively, while the peaks on other slope zones occur in March and November, with 36.9% and 30.1% on the slope zone above 20°, respectively. On the westward aspect, the greater the slope, the more abundant the snow cover is only observed in winter and early spring, but this pattern is not obvious on the different slope zones during snow accumulation and melting periods.

In a word, on the different aspect in the TP, mean SCF on the slope below 5° is the least, along with smoother intra-annual variations compared with other aspects. On the different slope zones, mean SCF on the northward aspect is the highest, while it is the lowest on the southward aspect and it is intermediate on the westward and eastward aspects with slightly higher mean SCF on the westward aspect than eastward aspect. Monthly mean SCF on the slope zones above 20° presents a unimodal distribution on the northward, eastward and westward aspects, while on the other aspect, it shows a bimodal distribution. On the different aspects, the higher the slope, the higher the SCF is observed in winter and early spring, but this pattern is not obvious on the different slopes during snow accumulation and melting periods.

Table 5. Monthly mean SCF (%) on the slope zones in the four aspects on the TP.

Aspect	Slope/°	Jan	Feb	Mar	Apr	May	Jun	Jul	Aug	Sep	Oct	Nov	Dec
Northward	0–5	17.2	17.7	17.4	16.0	16.2	9.2	2.0	2.9	8.2	22.2	21.1	15.0
	5–10	25.4	27.3	30.7	28.6	24.4	12.4	4.8	5.7	11.7	29.0	32.4	24.4
	10–20	33.4	34.5	37.6	33.6	25.7	13.1	6.5	7.1	12.9	29.2	36.8	32.5
	20–90	41.9	42.5	41.5	33.8	22.7	11.7	7.1	7.3	12.3	25.5	38.6	40.8
Eastward	0–5	16.3	17.8	17.6	15.5	15.0	8.5	2.1	2.9	7.3	19.8	19.4	13.8
	5–10	21.6	25.3	28.8	25.9	21.1	10.5	4.6	5.3	9.4	23.1	27.1	20.0
	10–20	24.9	28.7	32.8	29.1	21.7	10.9	5.6	6.0	9.9	21.9	28.5	23.7
	20–90	28.3	31.1	32.4	27.3	17.9	9.0	5.5	5.4	8.8	17.2	26.8	27.2
Southward	0–5	15.9	16.8	14.7	12.6	12.4	7.1	1.6	2.3	6.2	18.5	16.7	13.0
	5–10	16.8	20.3	22.4	20.5	17.5	8.9	3.3	4.0	7.5	18.2	20.2	14.6
	10–20	17.8	22.3	25.9	23.4	18.0	8.9	4.1	4.4	7.3	16.2	19.8	15.7
	20–90	19.4	24.1	26.4	23.0	15.8	8.1	4.7	4.6	7.1	12.7	18.0	17.3
Westward	0–5	18.4	19.2	17.8	15.3	14.7	7.7	1.9	2.6	7.1	19.9	20.6	15.6
	5–10	22.3	25.4	28.8	26.7	21.9	10.4	4.1	5.0	9.5	24.0	27.7	20.5
	10–20	25.8	29.4	34.1	31.4	23.5	11.2	5.3	5.9	10.4	23.8	29.7	24.3
	20–90	31.4	34.8	36.9	32.0	21.5	10.6	5.9	6.2	10.2	20.5	30.1	29.9

Preprints (www.preprints.org) | NOT PEER-REVIEWED | Posted: 3 July 2023 doi:10.20944/preprints202307.0030.v1

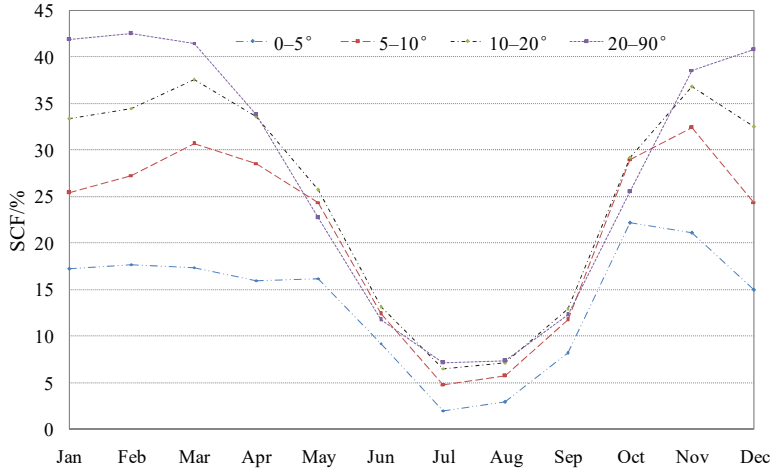

Figure 11. Monthly mean SCF on the slope zones in the north-facing aspect on the TP.

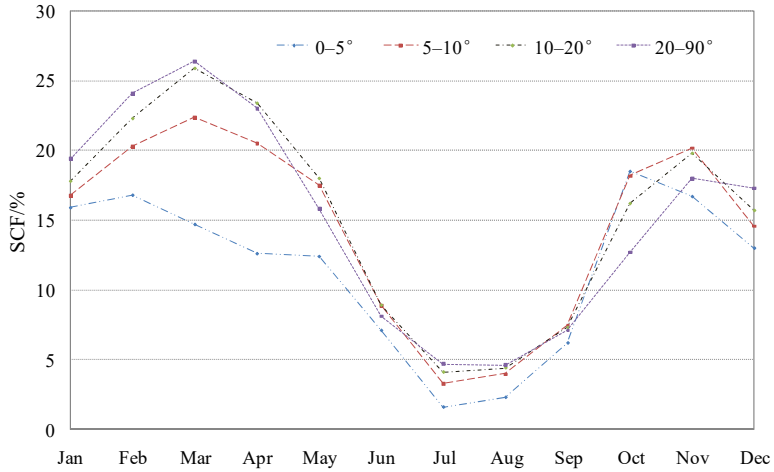

Figure 12. Monthly mean SCF on the slope zones in the south-facing aspect on the TP.

4. Discussion

Snow accumulation and loss is primarily controlled by atmospheric conditions, elevation and slope of the terrain. Atmospheric processes of interest are precipitation, deposition, condensation, turbulent transfer of heat and moisture, radiative exchange and air movement[23]. In the mountain regions, mountain ranges interrupt the winds and redistribute snow cover through snow drifting, slope and aspect influence incoming solar radiation and humidity, and latitude and elevation control air and ground temperature. The strong westerly winds blow the snow and tend to transfer snow into the valleys and decrease the total SCF [29]. Sublimation contributes largely to decreases in SCF during the winter, especial for the areas with thin snow cover [29][47]. More than half of snow mass was lost by sublimation in winter [47]. Distribution of the SCF over the mountainous areas varies with the terrain features, such as elevation, slope and aspect in the local areas, and the elevation of the terrain has a decisive role in snow accumulation. The spatiotemporal changes of snow cover in the mountain region have strong altitude dependence, which is related to variations in radiation and energy balances, and potentially to different accumulation regimes caused by windward/leeward effects [21-22].

Topography has a major effect on weather and climate in the Himalayas, and elevation and aspect therefore play important roles in the snow cover distribution [23-24]. Snow cover changes in Hindu Kush Himalaya (HKH) regions are highly variable temporally because of various types of

 doi:10.20944/preprints202307.0030.v1

controlling factors, including topographic effects, glacier dynamics, various types of geomorphological parameters, and generally shows altitudinal dependent [24] and the change in snow cover with altitude clearly shows a sharp jump in snow cover percent between 5001 and 6400m in elevation [26], which is consistent with hypsographic curve shown in Figure 5. The spatiotemporal snow cover variability across the HKH region is strongly influenced by topography because the topography has a strong effect on snow accumulation and melting [23][25].

The spatial distribution of snow cover on the TP is strongly controlled by the interactions between complex terrains and available moisture sources [12][20] [29-30][48]. The most persistent snow is located on the southern and western edges and the spatial distribution of snow cover on the TP corresponds well with the high mountains, including the Kunlun, Karakoram, Himalaya, Qilian, and Tanggula mountain ranges [47-54], which is consistent with findings from this study. Snow cover on the TP shows altitudinal dependence and the length of the snow covered season appears to be decreasing at lower elevation because of the increase in air temperatures. However, at higher elevations the increase in precipitation appears to compensate for the increase in air temperature such that the snow-free period has decreased. Snow cover distribution is generally precipitation-driven at high elevation sites but temperature-driven in the low altitudes [27].

In addition, the south-facing aspects receive more solar radiation and have higher temperature, which is not favor of snow cover and accumulation on the surface, causing that the leas mean SCF is observed on the south-facing aspects. However, due to mountain shadowing effects, the north-facing areas receives less insolation and solar radiation, along with lower temperature and sublimation associated, making snowmelt slower and longer snow cover duration. Therefore, the highest mean SCF is found in the north-facing aspects. The spatial distribution of snow cover on the TP generally shows that the higher SCF corresponds well with the high mountain ranges and strong elevation dependence.

5. Conclusion

The overall spatial distribution of snow cover on the TP and the impact of topographic factors (elevation, slope and aspect) on snow cover distribution are analyzed based on MODIS snow cover products and DEM using GIS spatial analysis techniques. Main results achieved are as follows：

(1) Snow cover on the TP is spatially very uneven and is generally characterized by rich snow and high SCF in the surrounding and interior high mountains, and less snow and low SCF in the inland basins and river valleys. The Nyainqentanglha and its eastward extending mountain ranges in southeastern Tibet, and the high mountain regions in the northwestern TP comprised of Karakoram, western Kunlun and western Himalayas, are two regions that have the highest SCF in the TP. Whereas, Qaidam basin in the north and southern Tibet valleys are two areas with the least SCF. Annual mean SCF on the TP is 15.7%, with same snow cover rates in spring and winter (21%), followed by autumn (17.5%), and the least in summer (5.4%).

(2) Snow cover on the TP shows strong elevation dependence with the higher the altitude, the higher the SCF, the longer the snow cover duration, and the more stable the intra-annual variation. In the TP, the high mountain and low-altitude regions are in good agreement with more and less SCF. In the areas below 3 km altitude, mean SCF is less than 4%, while it reaches 76.8% above 6 km altitude. In the areas below 4 km altitude, intra-annual variation of snow cover shows a unimodal distribution, while in the areas above 4 km altitude, intra-annual variation of snow cover presents a bimodal distribution. At altitudes below 6 km, the lowest SCF occurs in summer, whereas above 6 km it occurs in winter.

(3) Mountain slope is another important topographic factor affecting spatial distribution of snow cover in the TP. In the four slope zones, annual mean SCF on the slope zone below 5° is the lowest (12.7%), while on the slope above 20° it reaches 21.0% as the highest value. The intra-annual variation of snow cover on different slope zones presents a bimodal distribution pattern, and snow cover increases with slope in months of winter and spring, but it is not noticeable in other months.

(4) Mountain aspects influence spatial distribution of snow cover on the plateau through changing hydrothermal conditions between land and atmosphere on the TP. Snow cover on the

north-facing slope is the highest due to receiving less solar radiation and low temperature, while it is the lowest on the south-facing slope under strong insolation and higher temperature. Snow cover on the flat terrain without orientation of slope is less than that with aspects and its intra-annual variation shows a unimodal distribution. Sublimation under strong insolation due to the low latitude and increased sublimation of snow associated with the high wind greatly contributes to decreases in snow cover on the TP, especially during the winter season.

(5) The accuracy of remote sensing snow cover product is particularly important to capture a clear picture of spatiotemporal snow cover condition in the mountain regions. Previous study shows that the accuracy of MOD10A2 is over 90% under clear-sky condition. In this study, MODIS v005 is used and accuracy evaluation made previously is also based on the MODIS v005. Currently, MODIS v006 and v061 were developed and released to public use. However, there is a lack of systematic accuracy evaluation for latest MODIS products (v006 and v061). Our preliminary accuracy assessment shows that MODIS products(v006) and (v061) tend to overestimate snow cover on the TP and it is visually found that many water body such rivers on the TP are misidentified as snow cover pixels, which are largely due to NDSI > 0 used for snow cover mapping algorithm in latest versions of MODIS products. Therefore, accuracy evaluation of MODIS v006 and its latest version should be carried out carefully on the TP, and more consistent and longer time-series MODIS snow cover products are expected to be developed for use in the future.

Author Contributions: D.C. processed data and wrote the manuscript; L.L. and Z.W. reviewed and edited the manuscript. All authors have read and agreed to the published version of the manuscript.

Funding: This research work was financially supported by the Second Tibetan Plateau Scientific Expedition and Research (STEP) programme (2019QZKK0603;2019QZKK010312), Major Science & Technology programme of Tibet Autonomous Region (XZ202201ZD0005G01), and the National Natural Science Foundation of China (41561017).

Acknowledgments: The authors would like to acknowledge the U.S. National Snow and Ice Data Center (NSIDC) for providing the MODIS snow cover product (MOD10A2).

References

1. Barnett: T. P.; Adam, J. C.; Lettenmaier, D. P. Potential impacts of a warming climate on water availability in snow-dominated regions. *Nature* **2005**, 438, 303–309.
2. Armstrong, R. L.; Brodzig, M. J. Recent Northern Hemisphere snow extent: a comparison of data derived from visible and microwave satellite sensors. *Geophys. Res. Lett.* **2001**,28, 3673–3676.
3. Allchin, M. I.; Déry, S. J. A spatio-temporal analysis of trends in Northern Hemisphere snow-dominated area and duration, 1971–2014. *Ann. Glaciol.* **2017**, 58, 21–35.
4. Brown, R. D.; Robinson, D. A. Northern Hemisphere spring snow cover variability and change over 1922–2010 including an assessment of uncertainty. *The Cryosphere*, **2011**, 5(1), 219–229.
5. Déry, S. J.; Brown, R.D. Recent Northern Hemisphere snow cover extent trends and implications for the snow-albedo feedback. *Geophys. Res. Lett.* **2007**, 34(22), 60–64.
6. Choi, G.; Robinson, D. A.; Kang, S. Changing Northern Hemisphere snow seasons. *J. Clim.* **2010**, 23(19), 5 305–5 310.
7. Savoie, M. H.; Armstrong, R. L.; Brodzik, M. J.; et al. Atmospheric corrections for improved satellite passive microwave snow cover retrievals over the Tibet Plateau. *Remote Sens. Environ.* 2009,113, 2661–2669.
8. Yao, T.; Thompson, L.; Yang, W.; et al. Different glacier status with atmospheric circulations in Tibetan Plateau and surroundings. *Nat. Clim. Change*, **2012**, 2, 663–667.
9. Immerzeel, W.W.; Van Beek, L. P. H.; Bierkens, M. F. P. Climate change will affect the Asian water towers. *Science* **2010**, 328, 1382–1385.
10. Li, X.; Long, D.; Scanlon, B. R. et al. Climate change threatens terrestrial water storage over the Tibetan Plateau. *Nat. Clim. Change*, **2022**, 12, 801–807.
11. Ueno, K.; Tanaka, K.; Tsutsui, H.; et al. Snow cover conditions in the Tibetan Plateau observed during the winter of 2003/2004. *Arct. Antarct. Alp Res.* **2007**, 39(1),152–164.
12. Pu, Z.; Xu, L.; & Salomonson, V. V. MODIS/Terra observed seasonal variations of snow cover over the Tibetan Plateau. *Geophys. Res. Lett.* **2007**,34 (6),137–161.

13. Immerzeel, W. W.; Droogers, P.; De Jong, S. M.; et al. Large-scale monitoring of snow cover and runoff simulation in Himalayan river basins using remote sensing. *Remote Sens. Environ.* **2009**,113(1), 40–49.
14. Li, W.; Guo, W.; Qiu, B.; et al. Influence of Tibetan Plateau snow cover on East Asian atmospheric circulation at medium-range time scales. *Nat. Commun.* **2018**, 9,4243.
15. Liu, Y. M.; Bao, Q.; Duan, A. M.; et al. Recent progress in the impact of the Tibetan Plateau on climate in China. *Adv. Atmos. Sci.* **2007**, 24(6),1060–1076.
16. Duan, A. M.; Wu, G. X.; Liu, Y. M.; et al. Weather and climate effects of the Tibetan Plateau. *Adv. Atmos. Sci.* **2012**, 29(5), 978–992.
17. Yao, T.; Bolch, T.; Chen, D.; et al. The imbalance of the Asian water tower. *Nat. Rev. Earth Environ.* **2022**, 3, 618–632.
18. Nie, Y.; Pritchard, H. D.; Liu, Q.; et al. Glacial change and hydrological implications in the Himalaya and Karakoram. *Nat. Rev. Earth Environ*, **2021**, 2, 91–106.
19. Immerzeel, W. W.; Lutz, A. F.; Andrade, M.; et al. Importance and vulnerability of the world's water towers. *Nature* **2020**, 577, 364–369.
20. You, Q.; Wu, T.; Shen, L.; et al. Review of snow cover variation over the Tibetan Plateau and its influence on the broad climate system. *Earth Sci. Rev.* **2020**, 201,103043.
21. Li, Y.; Chen, Y.; Li, Z. Climate and topographic controls on snow phenology dynamics in the Tienshan Mountains, Central Asia. *Atmos. Res.* **2020**,236, 104813.
22. Tong, J.; Déry, S. J.; Jackson, P. L. Topographic control of snow distribution in an alpine watershed of western Canada inferred from spatially-filtered MODIS snow products. *Hydrol. Earth Syst. Sci.* **2009**, 13, 319–326.
23. Jain, S.; Goswami, A.; Saraf, A. Role of elevation and aspect in snow distribution in Western Himalaya. *Water Resour. Manag.* **2009**, 23(1),71–83.
24. Shrestha, A.; Agrawal, N.; Alfthan, B.; et al. The Himalayan Climate and Water Atlas. ICIMOD. **2015**.
25. Gurung, D. R.; Maharjan, S. B.; Shrestha, A. B.; et al., Climate and topographic controls on snow cover dynamics in the Hindu Kush Himalaya. *Int. J. Climatol.* **2017**, 37,3873–3882.
26. Desinayak, N.; Prasad, A. K.; El-Askary H.; et al. Snow cover variability and trend over the Hindu Kush Himalayan region using MODIS and SRTM data. *Ann. Geophys.* **2022**, 40(1),67–82.
27. Gao, J.; Williams, M. W.; Fu, X. D.; et al., Spatiotemporal distribution of snow in eastern Tibet and the response to climate change. *Remote Sens. Environ.* **2012**, 121, 1–9.
28. Chu, D. Spatiotemporal variability of snow cover on Tibet, China using MODIS remote-sensing data, *Int. J. Remote Sens.* **2018**, 39(20), 6784-6804.
29. Pu, Z.; Xu, L. MODIS/Terra observed snow cover over the Tibet Plateau: distribution, variation and possible connection with the East Asian Summer Monsoon (EASM). *Theor. Appl. Climatol.* **2009**,97,265–278.
30. Basang, D.; Barthel, K.; & Olseth, J. Satellite and ground observations of snow cover in Tibet during 2001–2015. *Remote Sens.* **2017**,14, 9 (11): 1201. doi:10.3390/rs9111201
31. Cai, D.; Guo, N.; Wang, X.; et al. The spatial and temporal variations of snow cover over the Qilian Mountains based on MODIS data. *Journal of Glaciology and Geocryology*, **2009**, 31(6), 1028–1036.
32. Yang, C. J.; Zhao, Z. J.; Ni, J.; et al. Temporal and spatial analysis of changes in snow cover in western Sichuan based on MODIS images. *Sci. China Earth Sci.* **2011**, 41(12),1743–1750.
33. Lou, M. Y.; Liu, Z. H.; Lou, S. M.; et al. Temporal and spatial distribution of snow cover in Xinjiang from 2002 to 2011. *Journal of Glaciology and Geocryology*,**2013**,35(5), 1095–1102.
34. Lin, J. T.; Feng, X. Z.; Xiao, P. F.; et al. Spatial and temporal distribution of snow cover in mountainous area of Manasi River Basin based on MODIS. *Remote Sensing Technology and Application*, **2011**, 26(4),469–475.
35. Dou, Y.; Chen, X.; Bao, A. M.; et al. Study of the temporal and spatial distribute of the snow cover in the Tianshan Mountains, China. *Journal of Glaciology and Geocryology*,**2010**, 32(1),28–34.
36. Lin, J. T.; Feng, X. Z.; Xiao, P. F.; et al. The spatial and temporal variations of snow cover over the Qilian mountains based on MODIS data. *Journal of Glaciology and Geocryology*, **2011**, 33(5), 971–978.
37. Körner, C.; Jetz, W.; Paulsen, J.; et al. A global inventory of mountains for bio-geographical applications. *Alpine Bot.* 2017,127, 1–15.
38. Zhang, Y. L.; Li, B. Y.; Zheng, D. A discussion on the boundary and area of the Tibetan Plateau in China. *Geographical Research*, **2002**, 21(1),1–8.
39. Sun, H. L.; Zheng, D. Formation, Evolution and Development of Qinghai-Xizang (Tibetan) Plateau (in Chinese). Guangdong Science & Technology Press, **1998**, 231–296.

40. Hall, D. K.; Riggs, G. A.; Salomonson, V. V.; et al. MODIS snow-cover products. *Remote Sens. Environ.* **2002**, 83,181–194.
41. Hall, D. K.; Riggs, G. A.; Foster, J. L.; et al. Development and evaluation of a cloud-gap-filled MODIS daily snow-cover product. *Remote Sens. Environ.* **2010**,114(3),496–503.
42. Klein, A. G.; Barnett, A. C. Validation of daily MODIS snow cover maps of the Upper Rio Grande River basin for the 2000-2001 snow year. *Remote Sens. Environ.* **2003**, 86,162–176.
43. Liang, T.; Zhang, X.; Xie, H.; et al. Toward improved daily snow cover mapping with advanced combination of MODIS and AMSR-E measurements. *Remote Sens. Environ.* **2008**, 112, 3750–3761.
44. Huang, X.; Liang, T.; Zhang, X.; et al. Validation of MODIS snow cover products using Landsat and ground measurements during the 2001–2005 snow seasons over northern Xinjiang, China. *Int. J. Remote Sens.* **2011**,*32*(1), 133-152.
45. Wang, X.; Xie, H.; Liang, T. Evaluation of MODIS snow cover and cloud mask and its application in Northern Xinjiang, China. *Remote Sens. Environ.* **2008**,112(4),1497–1513.
46. Li, J.; Zheng, B.; Yang, X.; et al. Glaciers in Tibet (in Chinese). Beijing: Science Press, 1986.
47. Qin, D.; Liu, S.; & Li, P. Snow cover distribution, variability, and response to climate change in western China. *J. Clim.* **2006**, 19, 1820–1833.
48. Shrestha**,** A**.** B**.;** Joshi**,** S**.** P**.;** Snow cover and glacier change study in Nepalese Himalaya using remote sensing and geographic information system. *Journal of Hydrology & Meteorology*, **2009**,6(1), 26-36.
49. Lhakpa, D.; Fan, Y.; Cai, Y. Continuous Karakoram glacier anomaly and its response to climate change during 2000–2021. *Remote Sens.* **2022**, 14, 6281.
50. Huang, X. D.; Deng, J.; Wang, W.; et al. Impact of climate and elevation on snow cover using integrated remote sensing snow products in Tibetan Plateau. *Remote Sens. Environ.* **2017**, 190, 274-288.
51. Bhattacharya, A.; Bolch, T.; Mukherjee, K.; et al. High Mountain Asian glacier response to climate revealed by multi-temporal satellite observations since the 1960s. *Nat. Commun.* **2021**,12, 4133.
52. Chen, X.; Long, D.; Liang, S.; et al. Developing a composite daily snow cover extent record over the Tibetan Plateau from 1981 to 2016 using multisource data. *Remote Sens. Environ.* **2018**, 215,284-299.
53. Choudhury, A.; Yadav, A. C.; Bonafoni, S. A response of snow cover to the climate in the Northwest Himalaya (NWH) using satellite products. *Remote Sens.* **2021**, 13, 655.
54. Tang, B. H.; Shrestha, B.; Li, Z. L.; et al. Determination of snow cover from MODIS data for the Tibetan Plateau region. *Int. J. Appl. Earth Obs.* **2012**, 21, 356–365.